Modelling the spatial crosstalk between two biochemical signals explains wood formation dynamics and tree-ring structure

Félix Hartmann, Cyrille Rathgeber, Eric Badel, Meriem Fournier, Bruno Moulia

Modelling the spatial crosstalk between two biochemical signals explains wood formation dynamics and tree-ring structure

Félix P. Hartmann[1],*, Cyrille B. K. Rathgeber[2], Éric Badel[1], Meriem Fournier[2], and Bruno Moulia[1]

[1] Université Clermont Auvergne, INRAE, PIAF, 63000 Clermont-Ferrand, France

[2] Université de Lorraine, AgroParisTech, INRAE, Silva, 54000 Nancy, France

* Correspondence: felix.hartmann@inrae.fr

Highlight

A dynamic model indicates that two interacting signals (auxin, plus a cytokinin or the TDIF peptide) can drive wood formation dynamics and tree-ring structure development in conifers.

Abstract

In conifers, xylogenesis during a growing season produces a very characteristic tree-ring structure: large, thin-walled earlywood cells followed by narrow, thick-walled latewood cells. Although many factors influence the dynamics of differentiation and the final dimensions of xylem cells, the associated patterns of variation remain very stable from one year to the next. While radial growth is characterized by an S-shaped curve, the widths of xylem differentiation zones exhibit characteristic skewed bell-shaped curves. These elements suggest a strong internal control of xylogenesis. It has long been hypothesized that much of this regulation relies on a morphogenetic gradient of auxin. However, recent modelling studies have shown that while this hypothesis could account for the dynamics of stem radial growth and the zonation of the developing xylem, it failed to reproduce the characteristic tree-ring structure. Here, we investigated the hypothesis of regulation by a crosstalk between auxin and a second biochemical signal, by using computational morphodynamics. We found that, in conifers, such a crosstalk is sufficient to simulate the characteristic features of wood formation dynamics, as well as the resulting tree-ring structure. In this model, auxin controls cell enlargement rates while another signal (e.g. cytokinin, TDIF) drives cell division and auxin polar transport.

Introduction

Tree radial growth relies on the production of new cells by the cambium and their subsequent differentiation. This process has a high level of plasticity, contributing to the ability of trees to acclimate to changing environmental conditions (Ragni and Greb, 2018). Therefore, in the current context of climate change, increasing attention is being paid to the influence of environmental factors on wood formation. However, the anatomical structure of conifer tree rings as revealed through tracheidograms, with their succession of large, thin-walled earlywood cells and narrow, thick-walled latewood cells, demonstrates a strikingly stable organization under contrasting conditions (Balducci *et al.*, 2016; Cuny *et al.*, 2018; Kiorapostolou *et al.*, 2018). Over one growing season, xylem radial growth generally follows a typical Gompertz curve, whose parameters depends on internal and external factors (Camarero *et al.*, 1998; Rossi *et al.*, 2003; Cuny *et al.*, 2012). The monitoring of wood formation by microcore samplings throughout the growing season reveals that the developing xylem generally displays a zonation pattern composed of (i) a division zone (or cambial zone *sensu stricto*), where cells grow and divide; (ii) an enlargement zone, where cells grow without dividing; (iii) a maturation zone, where non-growing cells undergo secondary wall deposition and wall lignification; and (iv) a mature zone, composed of dead, fully functional xylem cells (Wilson, 1984; Rathgeber *et al.*, 2016). Over the growing season, the width of each zone follows a specific skewed bell-shaped curve (Cuny *et al.*, 2013, 2014, 2015; Balducci *et al.*, 2016).

Although environmental influences are strong, the stability of these dynamic patterns over the growing seasons, and of the resulting tree-ring structure, suggests a tight internal control of xylem development. This becomes manifest when bark strips are removed (Brown and Sax, 1962; Li and Cui, 1988) or when cambial cells are placed into culture (Barnett, 1978). Then, growth becomes exponential and a callus is generally formed. This indicates that the internal control consists of either a radial field of mechanical pressure between the wood and the bark, or a flow of biochemical signals between the phloem and the xylem. The role played by several signals in the control of wood formation is well documented (see reviews in Fischer *et al.*, 2019 and Buttò *et al.*, 2020). Auxin, the most-studied phytohormone, is known to stimulate cell growth in many tissues, including stems (Perrot-Rechenmann, 2010), and to inhibit secondary cell wall deposition (Johnsson *et al.*, 2018). The radial distribution of auxin has been measured in several species and at different times and positions inside the forming wood during the growing season (Uggla *et al.*, 1996, 1998, 2001; Tuominen *et al.*, 1997). These measurements revealed a concentration peak around the cambial zone that varies in amplitude during the season. Based on these observations, some authors put forward the 'morphogen-gradient' hypothesis, according to which the graded concentration profile of auxin prescribes the width of each zone and, eventually, the final sizes of the xylem cells

produced (Sundberg *et al.,* 2000; Bhalerao and Bennett, 2003) by specifying the successive developmental identities of the cells (division and enlargement).

Computational morphodynamics is a powerful tool for testing the validity of such biological hypotheses, since it simulates the development of tissues and organs over space and time (Chickarmane *et al.,* 2010). This approach has shown that while the morphogen-gradient hypothesis accounts for the shape of the xylem radial-growth curve and for the seasonal dynamics of the developing xylem zonation, it fails to explain the final dimensions of the produced tracheids and the final structure of the annual ring (Hartmann *et al.,* 2017). As long as it is assumed that a single signal sets both division and enlargement identities—the core of the morphogen-gradient hypothesis—tracheid dimension patterns do not follow the typical conifer tree-ring structure that is commonly observed. Another issue was the prediction of unrealistic regular spatial oscillations of high amplitudes in final cell sizes.

In parallel, several models of tree-ring formation have focused on carbon and water resources (Deleuze and Houllier, 1998; Vaganov *et al.,* 2006, 2011; Hölttä *et al.,* 2010; Drew and Downes, 2015; Schiestl-Aalto *et al.,* 2015; Wilkinson *et al.,* 2015). However, these models all aim to establish relationships between environmental conditions and radial growth, while paying little attention to the biological mechanisms involved at the cellular level. More recently, Cartenì *et al.* (2018) developed an original functional approach and proposed a mechanism linking the seasonal variations in sugar availability in the cambium to the anatomical structure of tree rings. This model convincingly reproduces the typical conifer tree-ring structure, but does not fully represent the biological mechanisms underlying tracheid differentiation, since primary and secondary wall deposition are not distinguished. Another strong limitation is that cells grow independently of each other, making the model unable to capture the coordination of the processes of xylogenesis at the tissue scale.

While carbon and water availabilities are indispensable for wood formation, a growing body of experimental work points to the driving role played by hormones and peptides in this process (Etchells *et al.,* 2015; Gursanscky *et al.,* 2016; Immanen *et al.,* 2016; Brackmann *et al.,* 2018; Han *et al.,* 2018; Smetana *et al.,* 2019). Moreover, the stability of wood formation patterns, despite fluctuating environmental conditions, suggests an intrinsic regulatory action through biochemical signals, which is likely to be less sensitive than photosynthesis or water transport. Signals other than auxin are involved, such as TDIF (Tracheary Element Differentiation Inhibitory Factor), a CLE (CLAVATA/ESR-related) peptide which enters the cambium from the phloem and maintains vascular stem cells (Hirakawa *et al.,* 2008; Etchells *et al.,* 2015), or the plant hormone cytokinin, whose regulatory effect on cambial activity has been reported in aspen (Nieminen *et al.,* 2008). In addition, it has been observed that an increase in the cytokinin content leads to an increase in the cambial auxin concentration, probably through a change in auxin

transport (Immanen *et al.*, 2016). However, the full picture of the hormonal regulation of wood formation remains unclear, and morphodynamic models are needed to disentangle the role played by each signal. In the *Arabidopsis thaliana* root, for instance, Muraro *et al.* (2013, 2014) and el-Showk *et al.* (2015) developed models of vascular patterning based on a finding by Bishopp *et al.* (2011*a*) that a crosstalk between auxin and cytokinin specifies developmental zones. To reproduce maize leaf growth profiles, De Vos *et al.* (2020) integrated hormonal crosstalk into a model and predicted the existence of a signal produced in the mature part of the leaf. Following this line, we think that morphodynamic approaches will be instrumental in understanding xylogenesis, with the additional challenge that not only the growth profile and the developmental zonation have to be explained, but also the cell size pattern typical of tree rings.

To investigate the potential of the crosstalk between two biochemical signals in controlling tree radial growth, wood formation, and tree-ring structure, we further developed the XyDyS modelling framework to include the crosstalk between two morphogenetic signals (XyDyS2). Our central hypothesis in XyDyS2 is that the assignation of dividing, enlarging, and maturing cell identities is based on two biochemical signals. Auxin regulates cell growth, while another signal, identified as either TDIF or cytokinin, controls cell division. We also assume that this second signal acts on auxin transport. We used the XyDyS2 model to simulate the development of a radial cell file over a growing season and to assess the model's predictions against published experimental or observational data.

Materials and methods

Core of the XyDyS2 model

Taking advantage of the symmetry of the xylem tissue, we consider only a single radial file of differentiating cells (Fig. 1). The radial file is composed of cells that either differentiate into tracheids within a given growing season (possibly after one or several division cycles) or remain undifferentiated in the cambium at the end of the season. We focus on a single growing season and the formation of one tree ring. Spatially, the first boundary of the system (the 'cambium boundary') is the interface with the part of the cambium that differentiates into phloem. The second boundary (the 'xylem boundary') is the interface with the mature xylem produced during the previous year. Within a file, cells are indexed from $i=1$, at the cambium boundary, to $i=N(t)$, at the xylem boundary, $N(t)$ being the number of cells in the radial file at time t. Each cell is geometrically characterized by its radial dimension, called 'length' $L_i(t)$. $L(t)$ denotes the total length of the radial file at time t. For the initial condition, we suppose that there are initially N_0 cambial cells in the radial file, all with the same length L_{init}.
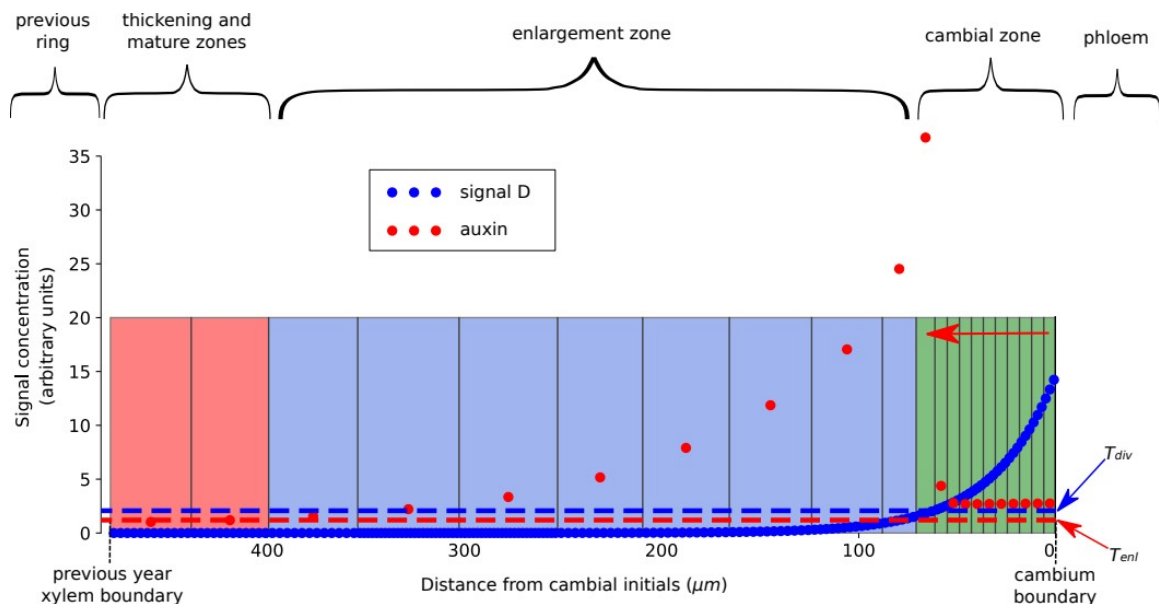
Fig. 1. *Schematic layout of a XyDyS simulation. Signal D and auxin form concentration gradients (blue and red dots, respectively), which determine cell identities and growth rates. Cells with a concentration of signal D above the division threshold (T_{div}, blue dashed line) have the ability to divide. Cells with a concentration of auxin above the enlargement threshold (T_{enl}, red dashed line) are growing, with a growth rate related to the auxin concentration. Carrier proteins transporting auxin toward the xylem are present only in cells that have the ability to divide. The zonation is based on cell identity and geometry. Cambial zone (green): small ($L_i < 2L_{init}$) growing cells. Enlargement zone (blue): large ($L_i > 2L_{init}$) growing cells. Thickening zone and mature zone (red): non-growing cells.*

Two signals, auxin and signal D, flow through the radial file, coming from the cambium boundary. Auxin is associated with cell growth, while signal D is associated with cell division (hence its name) and could be identified as either the TDIF peptide or the phytohormone cytokinin.

Apoplastic diffusion of signal D

The exact nature of signal D has not been elucidated, but we can assume that it diffuses in the apoplast, like peptides and cytokinins do (Robert and Friml, 2009). However, it has been shown that cytokinins also move through plasmodesmata, at least in Arabidopsis roots (Bishopp *et al.*, 2011*b*). This symplastic transport is different from the apoplastic transport but, from a modelling point of view, as long as passive diffusion is involved,

apoplastic transport can be a good approximation of symplastic transport if all cells have a similar size and if cells are small relative to the size of the whole organ, This is true for cambial cells, which are located where signal D is active.

The simplest model for signal diffusion is Fick's law (Crick, 1970), with a constant decay rate. We also assume that signal D is not produced in the developing tissue but comes from an external source at the cambium boundary. This 'source–diffusion–decay mechanism' is similar to that proposed by Wartlick *et al.* (2009) and Grieneisen *et al.* (2012) for root primary growth. Given the very slow growth of the developing xylem, dilution and advection (i.e. directed movement driven by tissue growth) can be neglected (Hartmann *et al.*, 2017). Then, the transport equation of signal D is written as:

$$\frac{\partial D(x,t)}{\partial t} = \underbrace{\delta_D \frac{\partial^2 D(x,t)}{\partial x^2}}_{diffusion} - \underbrace{\mu_D D(x,t)}_{decay}.$$

(1)

$D(x, t)$ denotes the concentration of signal D at position x and time t, δ_D denotes its diffusion coefficient, and μ_D denotes its decay rate. The space variable x is defined such that the cambium boundary of the file is located at $x=0$ and the xylem boundary is located at $x=L(t)$.

Equation 1 can be solved analytically. It is useful to introduce a characteristic length associated with the diffusion–decay process, expressed as:

$$\lambda = \sqrt{\frac{\delta_D}{\mu_D}}.$$

(2)

When the file becomes long compared with λ, the concentration profile reaches a stationary exponential shape, given by the equation:

$$D(x) = D(0) \exp\left(\frac{-x}{\lambda}\right).$$

(3)

This is a spatially continuous equation, since signal D diffuses along the continuous apoplasm. But, as for its biological effect, one may consider D_i, which denotes the average concentration of signal D in cell i. D_i can be easily calculated from Equations 1 and 3 knowing the position of the ith cell, $x_i(t)$, and its length, $L_i(t)$.

Symplastic polar transport of auxin

To describe the flow of auxin, we use a model of auxin fluxes similar to the 'unidirectional transport mechanism' from Grieneisen *et al.* (2012) and Hartmann *et al.* (2017). Where PIN-FORMED (PIN) carrier proteins are present, auxin is polarly transported from one cell to another. In addition to this active transport, there is a residual

constitutive permeability to auxin, which is the same between every consecutive cell. The auxin flux $F_{i,i+1}$ from cell i to cell $i+1$ depends on the concentration of auxin in cell i and on the amount of PIN in cell i oriented toward cell $i+1$ (Grieneisen *et al.*, 2012). This is written as:

$$F_{i,i+1}(t) = (p_{i,i+1}(t) + q) A_i(t).$$

(4)

$A_i(t)$ is the concentration of auxin in cell i, $p_{i,i+1}$ is the amount of PIN proteins in cell i oriented toward cell $i+1$, and q is the constitutive permeability to auxin. Moreover, we assume that PIN proteins are always oriented toward the xylem, that is, $p_{i,i-1}=0$. Therefore, auxin fluxes toward the cambium boundary rely only on constitutive permeability, that is, $F_{i,i-1}(t)=qA_i(t)$.

If one considers cell i, entering fluxes from cells $i-1$ and $i+1$ are respectively $F_{i-1,i}$ and $F_{i+1,i}$, and exiting fluxes toward cells $i-1$ and $i+1$ are respectively $F_{i,i-1}$ and $F_{i,i+1}$. Considering also decay, and dilution due to cell growth, the concentration of auxin in cell i is governed by the following equation:

$$\frac{dA_i}{dt} = \frac{1}{L_i} \left(\underbrace{F_{i-1,i} + F_{i+1,i}}_{entering fluxes} \underbrace{- F_{i,i-1} - F_{i,i+1}}_{exiting fluxes} \right) - \underbrace{\mu_A A_i}_{decay} - \underbrace{\dot{\epsilon}_i A_i}_{dilution}$$

(5)

μ_A is the decay rate of auxin, and $\dot{\epsilon}_i$ is the growth rate of cell i (Moulia and Fournier, 2009), defined by:

$$\dot{\epsilon}_i(t) = \frac{1}{L_i(t)} \frac{dL_i(t)}{dt}.$$

(6)

If the fluxes F are decomposed into their polar and passive components, Equation 5 becomes:

$$\frac{dA_i}{dt} = \frac{1}{L_i} \left((p_{i-1,i} + q) A_{i-1} - (p_{i,i+1} + 2q) A_i + q A_{i+1} \right) - \mu_A A_i - \dot{\epsilon}_i A_i.$$

(7)

Cell identity assignment

In the classical morphogen-gradient model (Bhalerao and Fischer, 2014; Hartmann *et al.*, 2017), cell identities are set by a single signal, with two concentration threshold values: a division threshold T_{div}, and an enlargement threshold T_{enl}, with $T_{div} > T_{enl}$. However, this way of assigning identities leads to unrealistic patterns in mature tracheid diameters (Hartmann *et al.*, 2017). Here, two distinct signals assign cell identities (Fig. 1). Where the concentration of signal D is higher than the division threshold T_{div}, cells are able to

divide. Similarly, where the concentration of auxin is higher than the enlargement threshold T_{enl}, cells enlarge. More formally, for a given cell:

- if $D_i \geq T_{div}$, the cell is able to enlarge and divide;
- if $D_i < T_{div}$ and $A_i \geq T_{enl}$, the cell is not able to divide any more, but it can keep enlarging;
- if $A_i < T_{enl}$, the cell no longer enlarges.

Moreover, to model the effect of signal D on auxin transport (Immanen *et al.*, 2016), we assume that auxin efflux carriers (PIN proteins) are present only in cells that are able to divide (i.e. $p_{i,i+1} > 0$ only if $D_i \geq T_{div}$), as most genes of the PIN family were found to be expressed much more strongly in dividing xylem cells than in expanding ones (Schrader *et al.*, 2003, Alonso-Serra *et al.*, 2019). Besides, in these cells, the amount of PIN proteins, $p_{i,i+1}$, is assumed to be proportional to the auxin concentration in cell *i*, as observed and modelled in the shoot apical meristem (Vieten *et al.*, 2005; Hartmann *et al.*, 2019):

$$p_{i,i+1}(t) = k_p A_i(t). \tag{8}$$

Cell growth and division

Although the mechanical force for cell enlargement comes from turgor pressure, this process is controlled by cell wall extensibility (Cosgrove, 2005). We assume that auxin acts on wall extensibility (Arsuffi and Braybrook, 2018) and thus controls the growth rate of enlarging cells. The simplest relationship is a direct proportionality: $\dot{\epsilon}_i(t) = k_g A_i(t)$, where k_g is a proportionality constant (Hartmann *et al.*, 2017). However, this relationship implies exponential growth for constant levels of auxin, which is unrealistic and tends to amplify inhomogeneities in cell sizes. Therefore, we propose here that larger cells show a weaker growth response to auxin, in the form of an inverse proportionality to cell size:

$$\dot{\epsilon}_i(t) = k_g \frac{L_{init}}{L_i(t)} A_i(t). \tag{9}$$

Cell division is modelled in a very classical and experimentally supported way and follows a simple geometrical criterion: if a cell has an identity that allows division, it divides when it reaches a critical length, defined as twice its initial length L_{init} (Hartmann *et al.*, 2017).

All parameters of the model are listed in Table 1.

Table 1: **Parameters of the model, with their values**

Symbol	Value	Unit	Description
N_0	6	Unitless	Initial number of cells in the file
L_0	6	μm	Initial size of the cells
T_d	2	Unitless	Division threshold
T_e	1.6	Unitless	Enlargement threshold
k_g	0.06	s^{-1}	Prefactor relating signal concentration to cell growth rate
δ_D	10	μm^2 s^{-1}	Diffusion coefficient of signal D
μ_D	10^{-2}	s^{-1}	Decay rate of signal D
μ_A	10^{-5}	s^{-1}	Decay rate of auxin
q	1.5×10^{-3}	μm s^{-1}	Permeability rate of the membranes to auxin
k_p	4×10^{-3}	Unitless	Proportionality coefficient between the concentration of auxin in a cell and the amount of PIN in the cell

Definition of developing zones

Experimentally, the descriptions of the developmental zones are based on visual criteria. In order to be able to compare the outputs of the XyDyS2 model with real data, we apply similar criteria *a posteriori* on model outputs, setting 'apparent statuses' to virtual cells:

- Cambial cells are growing cells that are smaller than twice the diameter of a newly created cell ($L_i < 2L_{init}$).

- Enlarging cells are growing cells that are larger than twice the diameter of a newly created cell ($L_i > 2L_{init}$).

- Wall-thickening and mature cells are cells that are no longer growing (Fig. 1).

Boundary conditions

The concentrations of auxin and signal D are imposed at the cambium boundary of the file, and are given as entries in the simulations (Fig. 2). The concentration of signal D at the cambium boundary is assumed to increase rapidly at the beginning of the season, and then decreases slowly. The concentration of auxin at the cambium boundary is assumed to peak during the first weeks of the season and then progressively decrease to zero as the season progresses. This reflects the sudden flush of auxin coming from the shoots during bud break. At the xylem boundary, we assume that the xylem acts as an impermeable barrier to molecules of auxin and signal D. Accordingly, a zero-flux boundary condition is imposed for both signals at the xylem boundary.
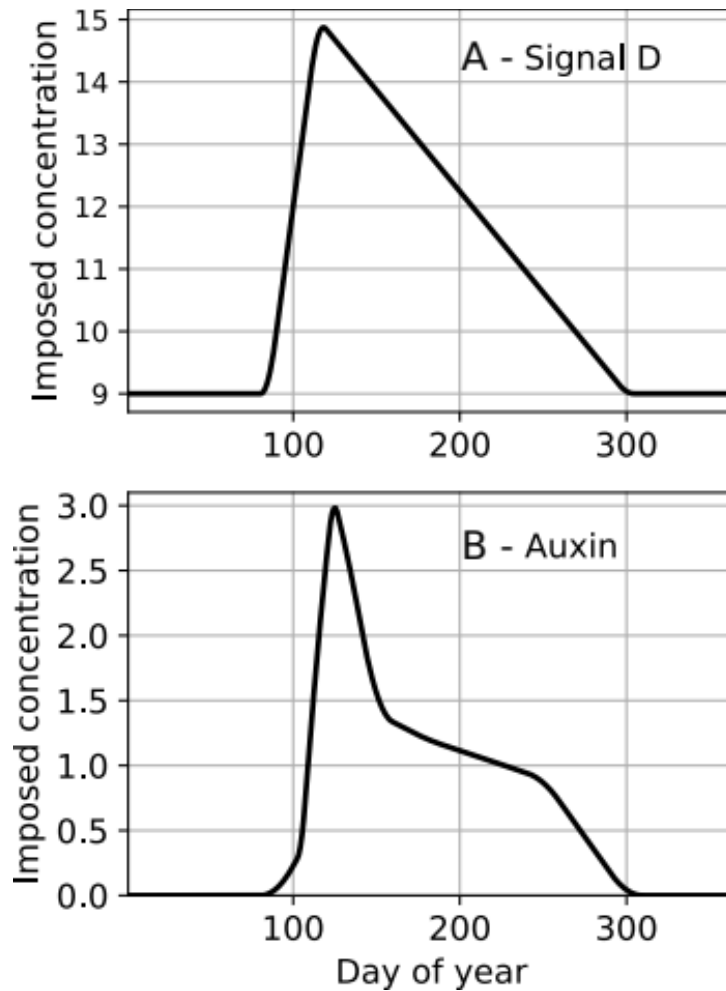
Fig. 2. *Concentrations of (A) signal D and (B) auxin imposed at the cambium boundary over a growing season.*

Implementation and visualization of the simulations

Transport equations are numerically solved using an explicit Euler method. For signal D, which diffuses in the apoplast, additional discretization nodes are regularly inserted in growing cells so that the Courant–Friedrichs–Lewy stability condition is always satisfied. We have developed a dedicated graphical user interface. The source code, written in Python, is freely available online (https://forgemia.inra.fr/felix.hartmann/xydys). Simulation outputs are visualized using the graphical convention explained in Fig. 1.

Results

Cross-talk between signal D and auxin leads to the progressive establishment of a stable auxin gradient

We first looked at the establishment of signal concentration profiles at the beginning of the growing season. Since the length of the cell file was initially shorter than the characteristic length λ, signal D was filling in the cell file, with a concentration higher than T_{div}, and hence T_{enl}, everywhere (Fig. 3A, Supplementary Video S1). Therefore, all cells were enlarging, dividing, and transporting auxin toward the xylem. As a consequence, auxin initially accumulated in the cells close to the xylem boundary, which thus had high growth rates. As the cell file became longer than λ, the concentration profile of signal D progressively reached the stationary exponential shape given by Equation 3. From this time on, polar auxin transport was limited to a few dividing cells and the concentration of auxin peaked around the boundary between the cambial and enlarging zones (Fig. 3B). The gradient of auxin was then stable and the height of the peak depended only on the auxin concentration at the cambium boundary. Near the end of the growing season, the auxin concentration at the cambium boundary had decreased (Fig. 2B) and the amount of auxin became too low for a peak to form (Fig. 3C). Altogether, this shows that active polar transport, regulated by another signal, can account for the peaked distribution of auxin observed experimentally in the developing xylem (Uggla *et al.*, 2001).
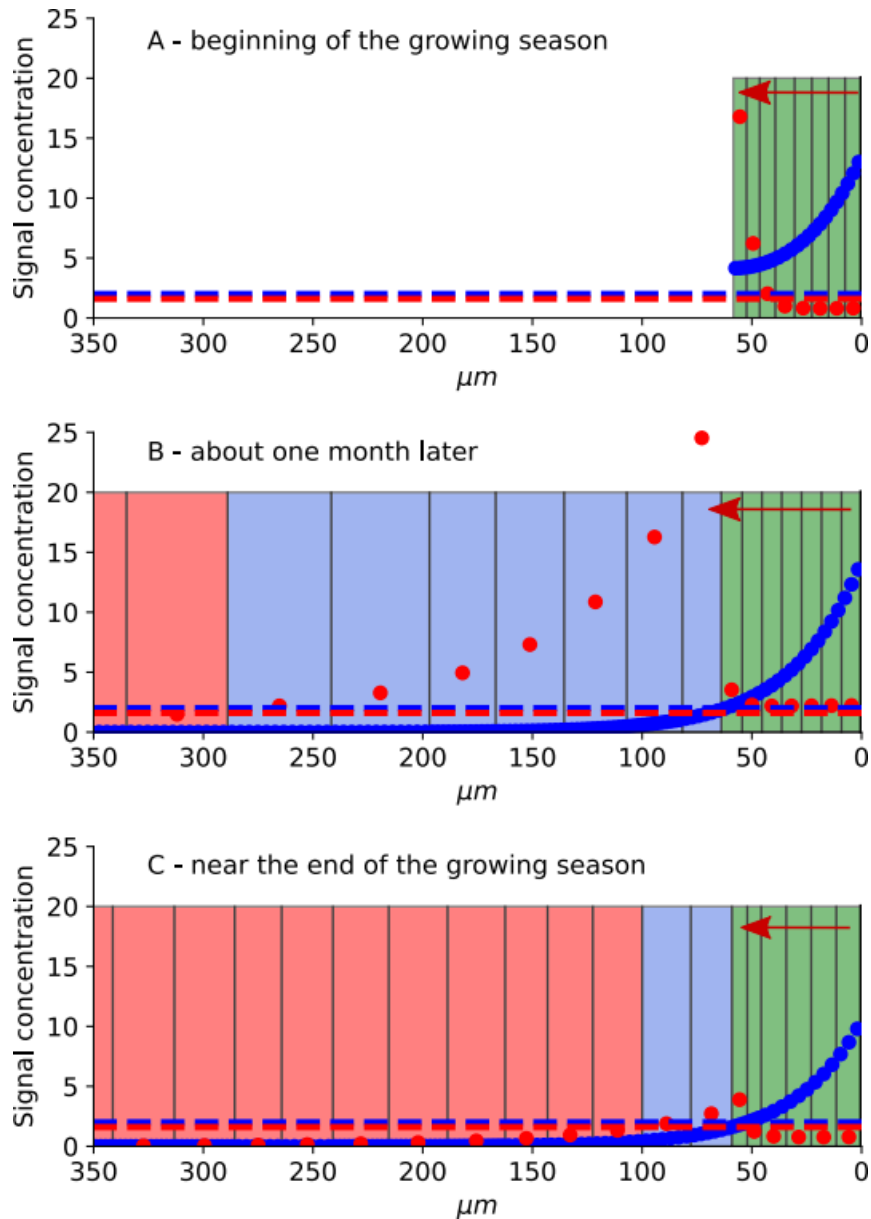
Fig. 3. *Establishment of signal gradients. (A) At the beginning of the growing season, signal D (blue dots) is above the division threshold (blue dashed line) in every cell. Auxin (red dots) is transported toward the xylem and accumulates at the xylem end of the cell file. (B) Approximately 1 month later, after the file has grown longer, both signals reach a stationary gradient. The auxin concentration peaks around the boundary between the cambial and enlargement zones. (C) Near the end of the growing season, the supply of signal is very low.*

Cross-talk between signal D and auxin controls the developmental zonation over the growing season

The width of the cambial zone was controlled mostly by signal D. At the beginning of the growing season, all cells belonged to the cambium, and the cambial zone expanded rapidly because signal D was high in every cell. This caused an early 'burst' in the number of cambial cells and, after a lag, in the number of enlarging cells. Such a rapid increase has been observed in studies monitoring real wood formation (Cuny *et al.*, 2014, 2018; Balducci *et al.*, 2016). As the concentration profile of signal D stabilized into a stationary gradient, the number of cambial cells reached a constant value. This value depended only on the concentration of signal D imposed at the cambium boundary and on the characteristic length, λ. Since λ was assumed to be constant (because the diffusion coefficient and decay rate of signal D are themselves constant), the width of the cambial zone was entirely driven by the concentration of signal D at the cambium boundary.

With regard to the enlargement zone, the width of the auxin gradient was the main driver. For a given value of the auxin decay rate, this width increased with the height of the concentration peak, which in turn depended on (i) the auxin concentration at the cambium boundary and (ii) the number of polar transporters in dividing cells. Since the number of transporters was assumed to be proportional to the local concentration of auxin, the width of the enlargement zone was entirely driven by the auxin concentration imposed at the cambium boundary.

The patterns of variations that we imposed on the concentrations of signal D and auxin at the cambium boundary, as described above, led to the variations in cell numbers in the cambial and enlargement zones represented in Fig. 4A. Comparison with experimental data from Cuny *et al.* (2014) showed good agreement along the growing season (Fig. 4B). This finding supports that developmental zonation can be adequately controlled by the cross-talk between two biochemical signals.
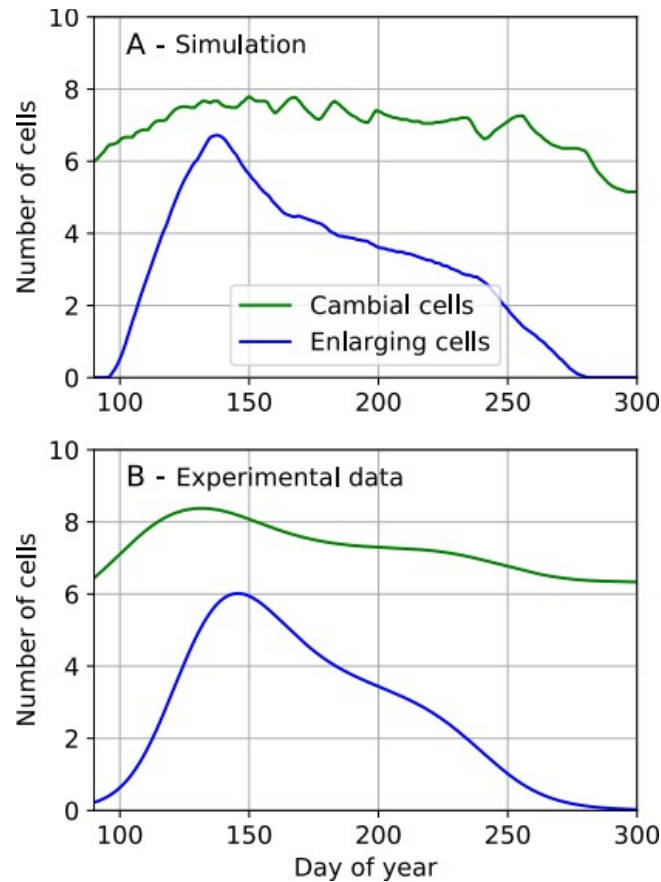
Fig. 4. Changes in the number of cambial and enlarging cells over a growing season. (A) As simulated by the XyDyS model. (B) From observations on silver firs (Abies alba) in the Vosges mountains (France), using data provided by Henri Cuny and published in Cuny et al. (2014).

Cross-talk between signal D and auxin engenders a realistic pattern of stem radial growth

The total growth rate of the cell file was directly related to the total quantity of auxin in the tissue. Three factors determined this quantity: (i) the concentration of auxin imposed at the cambium boundary; (ii) the number of cells contributing to polar auxin transport (i.e. the number of dividing cells), which was itself controlled by the gradient of signal D; and (iii) the amount of polar transporters in each of these cells ($p_{i,i+1}$), which was itself directly proportional to the local concentration of auxin. As a consequence, the global growth rate of the cell file was controlled in a highly non-linear way by the concentration of auxin at the cambium boundary and, to a lesser extent, by the boundary concentration of signal D.

With our hypotheses for the changes with time along the season of the concentrations of signal D and auxin at the cambium boundary, the simulation resulted in the cumulative growth curve shown in Fig. 5A. This curve can be compared with the measurements made on Scots pine (*Pinus sylvestris*) by Michelot *et al.* (2012) displayed in Fig. 5B. In our simulations, we did not try to match the final cumulative growth, which depends on many factors, so only the general shape of the curves should be compared. Although the agreement is not perfect, the simulated curve reproduces qualitatively the slow start, the progressive acceleration, the stable linear part, and the final progressive cessation of growth. However, the initial growth burst of the simulated curve is somewhat too pronounced, suggesting that other factors (e.g. water transport, sugar transport, or even temperature) may act as limiting factors at that time of the year.
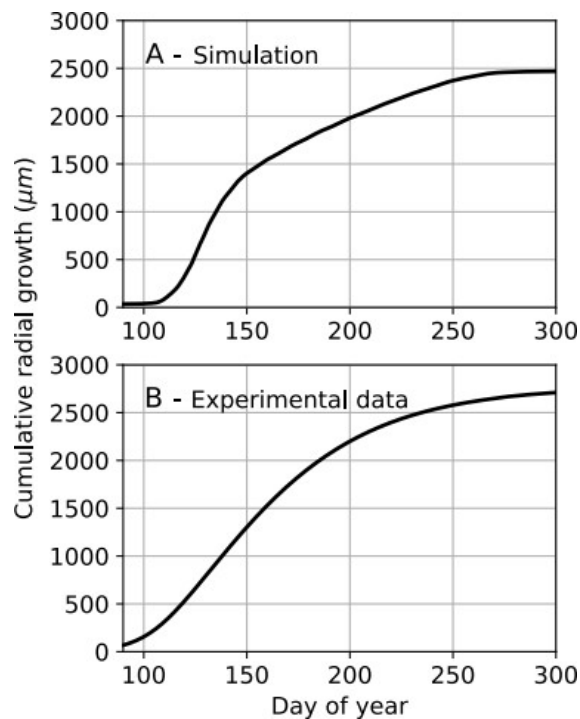

Fig. 5. *Cumulative radial growth of a tree ring. (A) As simulated by XyDyS. (B) As fitted from microcore measurements on Scots pines (P. sylvestris) growing in Fontainebleau forest, close to Paris (France), using data provided by Alice Michelot and published in Michelot et al. (2012).*

Cross-talk between signal D and auxin engenders a realistic tree-ring structure

We found that the final size of each tracheid was proportional to the height of the concentration peak of auxin at the time the cell lost its ability to divide. Indeed, the higher the peak was when the cell moves to the enlargement phase, the more auxin was

available to the cell for this phase. The height of the peak depended in turn on the concentration of auxin at the cambium boundary and on the magnitude of active polar transport. The strong supply of auxin at the beginning of the growing season resulted in large earlywood cells. The progressive decrease in auxin supply during the progression of the growing season led to transition wood and, finally, narrow latewood cells (Fig. 6A).
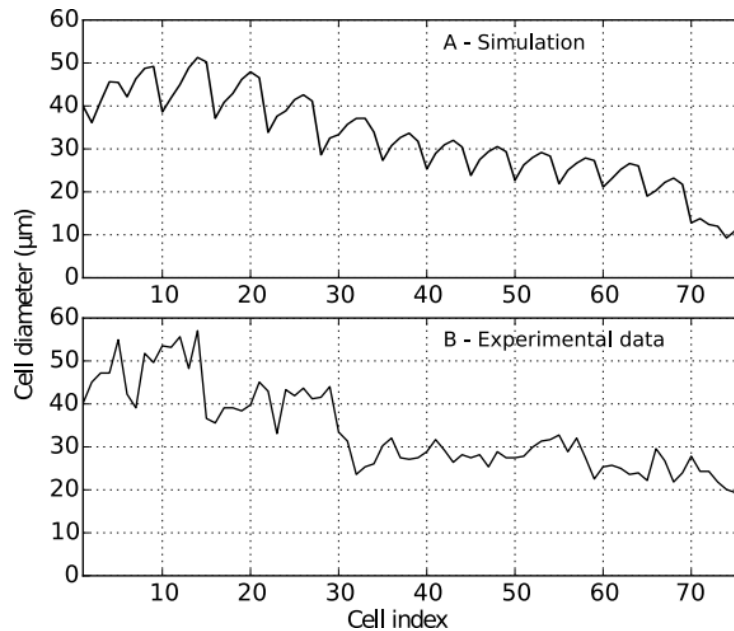

Fig. 6. Pattern of tracheid radial diameters along a mature tree ring. (A) As simulated by XyDyS. (B) As measured on a microcore of Scots pine (P. sylvestris) growing in the Vosges mountains (France). Data courtesy of Henri Cuny.

The previous implementation of the morphogen-gradient hypothesis—in which auxin acts as a single morphogenetic signal—in a dynamic model predicted unrealistic regular spatial oscillations of high amplitudes in final cell sizes (Hartmann *et al.,* 2017). Here, the size dependence between auxin concentration and growth rates introduced in Equation 9 largely alleviated this problem. This hypothesis did not produce smooth variations in cell sizes along a tracheidogram, but rather irregularities of moderate amplitude that can also be found in experimental data (Fig. 6B). Obviously, the experimental profile is rougher, due to secondary effects of other factors, but the trend is comparable.

Discussion

In a previous work (Hartmann *et al.,* 2017), we showed that the morphogen-gradient hypothesis was not compatible with the anatomical structure of conifer tree rings. Here, we propose a new model involving two biochemical signals. The first signal is associated with cell division and could be identified as the peptide TDIF, which is known to enter

the cambium from the phloem and to be involved in vascular stem cell maintenance (Hirakawa *et al.*, 2008; Etchells *et al.*, 2015). Another candidate for this first signal is the plant hormone cytokinin, whose regulatory effect on cambial activity has been reported in poplar (Nieminen *et al.*, 2008). The second signal is associated with cell growth and is identified as auxin.

Our model reproduced the main features of intra-annual dynamics of conifer wood formation over a growing season, that is, the shape of the radial growth curve (Fig. 5), the temporal evolution of differentiation zones (Fig. 4), and the final anatomical structure of the tree ring in terms of tracheid radial diameters (Fig. 6). It also provided an explanation for the pattern of auxin distribution in the developing xylem (Fig. 3 and Supplementary Video S1). In this model, the final radial size of cells is controlled by the supply of auxin to the cambium. In our previous model (Hartmann *et al.*, 2017), in which we considered a single signal (auxin) determining both cell division and growth, it was not possible to recreate the pattern of tracheid diameters. This became possible in XyDyS2 by introducing two new hypotheses: a decoupling of cell growth from division through the introduction of a second signal, plus a feedback of auxin on its own transport. With these new hypotheses, the final radial diameter of a tracheid was essentially set by its auxin content at the time it exits the cambial zone. This result supports the hypothesis of hierarchical control, according to which the cambial zone determines most of the next stages of xylem cell differentiation (Vaganov *et al.*, 2011).

Radial polar transport of auxin in the cambium

Our assumption that the radial polar transport of auxin plays a significant role in wood formation is based on experimental studies on aspen (Schrader *et al.*, 2003) and birch (Alonso-Serra *et al.*, 2019). Both studies reported that most genes of the *PIN* family have a higher expression in dividing xylem cells than in expanding ones. This is why we assumed that PIN proteins involved in lateral auxin transport are present only in dividing cells. However, there is no spatially resolved direct measurement of the concentration and orientation of PINs in the cambium. Our hypothesis that PINs are polarized toward the xylem remains therefore speculative. However, it provides a prediction that needs to be assessed experimentally. Another crucial hypothesis of our model is the auxin dependence of PIN synthesis. An auxin dependence of PIN synthesis is strongly supported by experiments on apical meristems (Vieten *et al.*, 2005), but so far there is no direct evidence of it in the cambium. Further experimental work is thus needed to gain a better understanding of polar auxin transport in the developing xylem and assess our hypotheses.

Cell size fluctuations and stochasticity

In our previous modelling work, we reported large oscillations of final cell sizes along a simulated tree ring, with a wavelength regularity of three to five cells (Hartmann *et al.*,

2017). This was amplified by the direct proportionality between auxin concentration and cell growth rate. We showed here that these oscillations can be strongly attenuated by assuming that the growth response of cells to auxin is size dependent. This assumption is based on the biological idea that larger cells have a lower density of DNA with respect to their cytoplasmic and cell wall volumes (the nucleocytoplasmic ratio; see review in Cantwell and Nurse, 2019) provided there is no endoreplication, and thus have a lower capacity to sustain growth in response to auxin. This hypothesis is supported by the work of Mellerowicz and Riding (1992), who did not find any endoreplication in *Abies balsamea* cambium. Further support for a weaker growth response in larger cells comes from observations in sepal epidermis, where smaller cell lineages grow faster than larger ones (Tsugawa *et al.*, 2017). This results in a homogenization of cell sizes. Moreover, in the shoot apical meristem of *A. thaliana*, Willis *et al.* (2016) found that, after an asymmetrical division, the smaller daughter cell grows at faster rate than the larger one.

Although attenuated, fluctuations in final cell sizes were still present in our simulations (Fig. 6). They were, however, similar in amplitude to fluctuations observed in actual tracheidograms. It is interesting to note that these oscillations are completely determined by the mechanisms behind the growth dynamics of the developing xylem tissue, without any explicit stochastic component. Numerous cellular processes involve a stochastic component (Meroz and Bastien, 2014; Meyer *et al.*, 2017), and this aspect should also be investigated in the future. Nevertheless, our results underline that not all heterogeneities in cell features are attributable to stochastic processes.

We used a purely deterministic criterion for division, based on a cell size threshold. This assumption is supported by the probable existence of a cell size checkpoint at the G1–S transition (Schiessl *et al.*, 2012). Moreover, analyses of cell size distribution along the growth zone of developing roots (Beemster and Baskin, 1998) and leaves (Fiorani *et al.*, 2000) suggest that all the cells in a given meristem divide in half at the same length. However, the critical-size criterion is likely to be essentially a first-order approximation. In the shoot apical meristem, Willis *et al.* (2016) found that it could not fully account for the cell-cycle statistics observed. Future modelling studies could explore whether introducing stochasticity here can better reproduce the wood anatomical structure.

Role of environmental factors

We focused on biochemical signals to model wood formation, with no explicit mention of environmental factors. In reality, the inputs of our model, that is, the supplies of signals into the cambium, are related to developmental and environmental conditions. These relationships are not known exactly, and tree-scale models are needed to connect signal sources to sinks. Moreover, temperature and water status also alter the capacity of cells to respond to signals. Here, we made the implicit hypothesis that environmental conditions were not limiting. Further developments of our model could consider how wood formation dynamics are affected by water stress, which can be a limiting factor at

least in the xeric area (Cabon *et al.*, 2020*a*). Ignoring the effects of temperature also limits the scope of our model. For instance, we did not model the timing of the onset of cambial activity, which is likely to be mainly triggered by temperature (Begum *et al.*, 2012; Delpierre *et al.*, 2019; Cabon *et al.*, 2020*b*). Similarly, growth cessation in autumn may involve responses to day length (Baba *et al.*, 2011), temperature (Begum *et al.*, 2016), or even drought (Ziaco *et al.*, 2016, Cabon *et al.*, 2020*b*). Finally, mechanical strains have been shown to be a major driver of wood growth rate (Bonnesoeur *et al.*, 2016; Niez *et al.*, 2019) and wood anatomy (Roignant *et al.*, 2018).

The final phases of xylem cell differentiation, that is, secondary wall formation and programmed cell death, involve many biochemical processes. However, they may not be controlled by an additional signal. It has been observed that the amount of secondary wall material is about the same in each mature xylem cell along a tree ring, except for the very last latewood cells (Cuny *et al.*, 2014). This observation could be used to deduce secondary wall thickness from cell size. In addition, temperature seems to play little role in wall thickness, since forming tracheids compensate a decreased rate of differentiation by an extended duration, except for the last latewood cells (Cuny *et al.*, 2018).

Role of mechanical signalling

Here, we considered that the spatial organization of the cambium relies only on biochemical signals. However, it is possible that the mechanical pressure exerted by the bark is also involved in cambial organization, by setting a radial polarity field (Yeoman and Brown, 1971). Mechanical signals are known to be essential in the dynamics of the shoot apical meristem, especially in the boundary region, where cells divide periclinally (Louveaux *et al.*, 2016) like in the cambium. While biochemical signals are likely to play a major role in controlling cell differentiation, division, and growth rate during the growing season, mechanical signals probably also provide cues to cambial cells.

General conclusion

Our results indicate a plausible hormonal regulatory system of wood formation. This model explains the characteristic features of wood formation dynamics and the pattern of tracheid diameters along a tree ring, and provides verifiable hypotheses on auxin transport in the cambium. It is limited to tracheids in conifers and is not directly applicable to hardwood, which consists of two cell types, fibres and vessels. Extending the model to this tissue will require additional rules for determining cell fate. Future, more advanced models of cambial activity and wood formation should also embrace environmental factors and mechanical signalling.

Supplementary data

Video S1: **Video of the simulation.**

Acknowledgements

Author contributions

FPH, CBKR, MF, and BM: Formalization; FPH: investigation, methodology, visualization, writing—original draft;

CBKR, EB, and BM: writing—review & editing.

All authors read and approved the final article.

Data availability

The source code of XyDyS is freely available online at https://forgemia.inra.fr/felix.hartmann/xydys.

The data supporting the findings of this study are available from the corresponding author, Félix P. Hartmann, upon request.

References

Alonso-Serra J, Safronov O, Lim KJ, et al. 2019. Tissue-specific study across the stem reveals the chemistry and transcriptome dynamics of birch bark. New Phytologist **222,** 1816–1831.

Arsuffi G, Braybrook SA. 2018. Acid growth: an ongoing trip. Journal of Experimental Botany **69,** 137–146.

Baba K, Karlberg A, Schmidt J, Schrader J, Hvidsten TR, Bako L, Bhalerao RP. 2011. Activity–dormancy transition in the cambial meristem involves stage-specific modulation of auxin response in hybrid aspen. Proceedings of the National Academy of Sciences, USA **108,** 3418–23.

Balducci L, Cuny HE, Rathgeber CB, Deslauriers A, Giovannelli A, Rossi S. 2016. Compensatory mechanisms mitigate the effect of warming and drought on wood formation. Plant, Cell & Environment **39,** 1338–1352.

Barnett JR. 1978. Fine structure of parenchymatous and differentiated *Pinus radiata* callus. Annals of Botany **42,** 367–373.

Beemster GT, Baskin TI. 1998. Analysis of cell division and elongation underlying the developmental acceleration of root growth in *Arabidopsis thaliana*. Plant Physiology **116,** 1515–1526.

Begum S, Kudo K, Matsuoka Y, et al. 2016. Localized cooling of stems induces latewood formation and cambial dormancy during seasons of active cambium in conifers. Annals of Botany **117,** 465–477.

Begum S, Nakaba S, Yamagishi Y, Yamane K, Islam MA, Oribe Y, Ko JH, Jin HO, Funada R. 2012. A rapid decrease in temperature induces latewood formation in artificially reactivated cambium of conifer stems. Annals of Botany **110,** 875–885.

Bhalerao RP, Bennett MJ. 2003. The case for morphogens in plants. Nature Cell Biology **5,** 939–943.

Bhalerao RP, Fischer U. 2014. Auxin gradients across wood – instructive or incidental? Physiologia Plantarum **151,** 43–51.

Bishopp A, Help H, El-Showk S, Weijers D, Scheres B, Friml J, Benková E, **Mähönen AP, Helariutta Y.** 2011a. A mutually inhibitory interaction between auxin and cytokinin specifies vascular pattern in roots. Current Biology **21,** 917–926.

Bishopp A, Lehesranta S, Vatén A, Help H, El-Showk S, Scheres B, Helariutta K, Mähönen AP, Sakakibara H, Helariutta Y. 2011b. Phloem-transported cytokinin regulates polar auxin transport and maintains vascular pattern in the root meristem. Current Biology **21,** 927–932.

Bonnesoeur V, Constant T, Moulia B, Fournier M. 2016. Forest trees filter chronic wind-signals to acclimate to high winds. New Phytologist **210,** 850–860.

Brackmann K, Qi J, Gebert M, et al. 2018. Spatial specificity of auxin responses coordinates wood formation. Nature Communications **9,** 875.

Brown CL, Sax K. 1962. The influence of pressure on the differentiation of secondary tissues. American Journal of Botany **49,** 683–691.

Buttò V, Deslauriers A, Rossi S, Rozenberg P, Shishov V, Morin H. 2020. The role of plant hormones in tree-ring formation. Trees **34,** 315–335.

Cabon A, Fernández-de-Uña L, Gea-Izquierdo G, Meinzer FC, Woodruff DR, Martínez-Vilalta J, De Cáceres M. 2020a. Water potential control of turgor-driven tracheid enlargement in Scots pine at its xeric distribution edge. New Phytologist **225,** 209–221.

Cabon A, Peters RL, Fonti P, Martínez-Vilalta J, De Cáceres M. 2020b. Temperature and water potential co-limit stem cambial activity along a steep elevational gradient. New Phytologist **226,** 1325–1340.

Camarero JJ, Guerrero-**Campo J,** Gutié**rrez E.** 1998. Tree-ring growth and structure of *Pinus uncinata* and *Pinus sylvestris* in the central Spanish Pyrenees. Arctic and Alpine Research **30,** 1–10.

Cantwell H, Nurse P. 2019. Unravelling nuclear size control. Current Genetics **65,** 1281–1285.

Cartenì F, **Deslauriers A, Rossi S, Morin H, De Micco V, Mazzoleni S, Giannino F.** 2018. The physiological mechanisms behind the earlywood-to-latewood transition: a process-based modeling approach. Frontiers in Plant Science **9,** 1053.

Chickarmane V, Roeder AH, Tarr PT, Cunha A, Tobin C, Meyerowitz EM. 2010. Computational morphodynamics: a modeling framework to understand plant growth. Annual Review of Plant Biology **61,** 65–87.

Cosgrove DJ. 2005. Growth of the plant cell wall. Nature Reviews. Molecular Cell Biology **6,** 850–861.

Crick F. 1970. Diffusion in embryogenesis. Nature **225,** 420–422.

Cuny HE, Fonti P, Rathgeber CBK, von Arx G, Peters RL, Frank DC. 2018. Couplings in cell differentiation kinetics mitigate air temperature influence on conifer wood anatomy. Plant, Cell & Environment **42,** 1222–1232.

Cuny HE, Rathgeber CB, Frank D, *et al.* 2015. Woody biomass production lags stem-girth increase by over one month in coniferous forests. Nature Plants **1,** 15160.

Cuny HE, **Rathgeber CB, Frank D, Fonti P, Fournier M.** 2014. Kinetics of tracheid development explain conifer tree-ring structure. New Phytologist **203,** 1231–1241.

Cuny HE, Rathgeber CB, Kiessé TS, **Hartmann FP, Barbeito I, Fournier M.** 2013. Generalized additive models reveal the intrinsic complexity of wood formation dynamics. Journal of Experimental Botany **64,** 1983–1994.

Cuny HE, Rathgeber CB, Lebourgeois F, Fortin M, Fournier M. 2012. Life strategies in intra-annual dynamics of wood formation: example of three conifer species in a temperate forest in north-east France. Tree Physiology **32,** 612–625.

De Vos D, Nelissen H, AbdElgawad H, Prinsen E, Broeckhove J, Inzé D, **Beemster GTS.** 2020. How grass keeps growing: an integrated analysis of hormonal crosstalk in the maize leaf growth zone. New Phytologist **225,** 2513–2525.

Deleuze C, Houllier F. 1998. A simple process-based xylem growth model for describing wood microdensitometric profiles. Journal of Theoretical Biology **193,** 99–113.

Delpierre N, Lireux S, Hartig F, *et al.* 2019. Chilling and forcing temperatures interact to predict the onset of wood formation in Northern Hemisphere conifers. Global Change Biology **25,** 1089–1105.

Drew DM, Downes G. 2015. A model of stem growth and wood formation in *Pinus radiata*. Trees **29,** 1395–1413.

el-Showk S, Help-Rinta-Rahko H, Blomster T, Siligato R, Marée AF, Mähönen AP, Grieneisen VA. 2015. Parsimonious model of vascular patterning links transverse hormone fluxes to lateral root initiation: auxin leads the way, while cytokinin levels out. PLoS Computational Biology **11,** e1004450.

Etchells JP, Mishra LS, Kumar M, Campbell L, Turner SR. 2015. Wood formation in trees is increased by manipulating PXY-regulated cell division. Current Biology **25,** 1050–1055.

Fiorani F, Beemster GT, Bultynck L, Lambers H. 2000. Can meristematic activity determine variation in leaf size and elongation rate among four *Poa* species? A kinematic study. Plant Physiology **124,** 845–856.

Fischer U, Kucukoglu M, Helariutta Y, Bhalerao RP. 2019. The dynamics of cambial stem cell activity. Annual Review of Plant Biology **70,** 293–319.

Grieneisen VA, Scheres B, Hogeweg P, M Marée AF. 2012. Morphogengineering roots: comparing mechanisms of morphogen gradient formation. BMC Systems Biology **6,** 37.

Gursanscky NR, Jouannet V, Grünwald K, Sanchez P, Laaber-Schwarz M, Greb T. 2016. *MOL1* is required for cambium homeostasis in Arabidopsis. The Plant Journal **86,** 210–220.

Han S, Cho H, Noh J, Qi J, Jung HJ, Nam H, Lee S, Hwang D, Greb T, Hwang I. 2018. BIL1-mediated MP phosphorylation integrates PXY and cytokinin signalling in secondary growth. Nature Plants **4,** 605–614.

Hartmann FP, Barbier de Reuille P, Kuhlemeier C. 2019. Toward a 3D model of phyllotaxis based on a biochemically plausible auxin-transport mechanism. PLoS Computational Biology **15,** 1–21.

Hartmann FP, Rathgeber CBK, Fournier M, Moulia B. 2017. Modelling wood formation and structure: power and limits of a morphogenetic gradient in controlling xylem cell proliferation and growth. Annals of Forest Science **74,** 14.

Hirakawa Y, Shinohara H, Kondo Y, Inoue A, Nakanomyo I, Ogawa M, Sawa S, Ohashi-Ito K, Matsubayashi Y, Fukuda H. 2008. Non-cell-autonomous control of vascular stem cell fate by a CLE peptide/receptor system. Proceedings of the National Academy of Sciences, USA **105,** 15208–15213.

Hölttä T, **Mäkinen H, Nöjd P, Mäkelä A**, **Nikinmaa E.** 2010. A physiological model of softwood cambial growth. Tree Physiology **30,** 1235–1252.

Immanen J, Nieminen K, Smolander OP, *et al.* 2016. Cytokinin and auxin display distinct but interconnected distribution and signaling profiles to stimulate cambial activity. Current Biology **26,** 1990–1997.

Johnsson C, Jin X, Xue W, Dubreuil C, Lezhneva L, Fischer U. 2018. The plant hormone auxin directs timing of xylem development by inhibition of secondary cell wall deposition through repression of secondary wall NAC-domain transcription factors. Physiologia Plantarum **165,** 673–689.

Kiorapostolou N, Galiano-Pérez L, von **Arx G, Gessler A, Petit G.** 2018. Structural and anatomical responses of *Pinus sylvestris* and *Tilia platyphyllos* seedlings exposed to water shortage. Trees **32,** 1211–1218.

Li Z, Cui K. 1988. Differentiation of secondary xylem after girdling. IAWA Journal **9,** 375–383.

Louveaux M, Julien J-D, **Mirabet V, Boudaoud A, Hamant O.** 2016. Cell division plane orientation based on tensile stress in *Arabidopsis thaliana*. Proceedings of the National Academy of Sciences, USA **113,** 4294–4303.

Mellerowicz EJ, Riding R. 1992. Does DNA endoreduplication occur during differentiation of secondary xylem and phloem in *Abies balsamea*? International Journal of Plant Sciences **153,** 26–30.

Meroz Y, Bastien R. 2014. Stochastic processes in gravitropism. Frontiers in Plant Science **5,** 674.

Meyer HM, Teles J, Formosa-**Jordan P, Refahi Y,** San-**Bento R, Ingram G,** Jö**nsson H, Locke JCW, Roeder AH.** 2017. Fluctuations of the transcription factor atml1 generate the pattern of giant cells in the *Arabidopsis* sepal. eLife **6,** e19131.

Michelot A, Simard S, Rathgeber C, Dufrêne E, Damesin C. 2012. Comparing the intra-annual wood formation of three European species (*Fagus sylvatica*, *Quercus petraea* and *Pinus sylvestris*) as related to leaf phenology and non-structural carbohydrate dynamics. Tree Physiology **32,** 1033–1045.

Moulia B, Fournier M. 2009. The power and control of gravitropic movements in plants: a biomechanical and systems biology view. Journal of Experimental Botany **60,** 461–486.

Muraro D, Byrne H, King J, Bennett M. 2013. The role of auxin and cytokinin signalling in specifying the root architecture of *Arabidopsis thaliana*. Journal of Theoretical Biology **317,** 71–86.

Muraro D, Mellor N, Pound MP, *et al.* 2014. Integration of hormonal signaling networks and mobile microRNAs is required for vascular patterning in *Arabidopsis* roots. Proceedings of the National Academy of Sciences, USA **111,** 857–62.

Nieminen K, Immanen J, Laxell M, *et al.* 2008. Cytokinin signaling regulates cambial development in poplar. Proceedings of the National Academy of Sciences, USA **105,** 20032–7.

Niez B, Dlouhá J, **Moulia B, Badel E.** 2019. Water-stressed or not, the mechanical acclimation is a priority requirement for trees. Trees **33,** 279–291.

Perrot-Rechenmann C. 2010. Cellular responses to auxin: division versus expansion. Cold Spring Harbor Perspectives in Biology **2,** a001446.

Ragni L, Greb T. 2018. Secondary growth as a determinant of plant shape and form. Seminars in Cell & Developmental Biology **79,** 58–67.

Rathgeber CB, Cuny HE, Fonti P. 2016. Biological basis of tree-ring formation: a crash course. Frontiers in Plant Science **7,** 734.

Robert HS, Friml J. 2009. Auxin and other signals on the move in plants. Nature Chemical Biology **5,** 325–332.

Roignant J, Badel É, Leblanc-Fournier N, Brunel-Michac N, Ruelle J, Moulia B, Decourteix M. 2018. Feeling stretched or compressed? The multiple mechanosensitive responses of wood formation to bending. Annals of Botany **121,** 1151–1161.

Rossi S, Deslauriers A, Morin H. 2003. Application of the Gompertz equation for the study of xylem cell development. Dendrochronologia **21,** 33–39.

Schiessl K, Kausika S, Southam P, Bush M, Sablowski R. 2012. Jagged controls growth anisotropy and coordination between cell size and cell cycle during plant organogenesis. Current Biology **22,** 1739–1746.

Schiestl-Aalto P, Kulmala L, Mäkinen H, Nikinmaa E, Mäkelä A. 2015. CASSIA–a dynamic model for predicting intra-annual sink demand and interannual growth variation in Scots pine. New Phytologist **206,** 647–659.

Schrader J, Baba K, May ST, Palme K, Bennett M, Bhalerao RP, Sandberg G. 2003. Polar auxin transport in the wood-forming tissues of hybrid aspen is under simultaneous control of developmental and environmental signals. Proceedings of the National Academy of Sciences, USA **100,** 10096–101.

Smetana O, Mäkilä R, **Lyu M**, *et al.* 2019. High levels of auxin signalling define the stem-cell organizer of the vascular cambium. Nature **565,** 485–489.

Sundberg B, Uggla C, Tuominen H. 2000. Cambial growth and auxin gradients. In: Savidge R, Barnett J, Napier R, eds. Cell and molecular biology of wood formation. Oxford: BIOS Scientific Publishers, 169–188.

Tsugawa S, Hervieux N, Kierzkowski D, Routier-Kierzkowska AL, Sapala A, Hamant O, Smith RS, Roeder AHK, Boudaoud A, Li CB. 2017. Clones of cells switch from reduction to enhancement of size variability in Arabidopsis sepals. Development **144,** 4398–4405.

Tuominen H, Puech L, Fink S, Sundberg B. 1997. A radial concentration gradient of indole-3-acetic acid is related to secondary xylem development in hybrid aspen. Plant Physiology **115,** 577–585.

Uggla C, Magel E, Moritz T, Sundberg B. 2001. Function and dynamics of auxin and carbohydrates during earlywood/latewood transition in scots pine. Plant Physiology **125,** 2029–2039.

Uggla C, Mellerowicz EJ, Sundberg B. 1998. Indole-3-acetic acid controls cambial growth in scots pine by positional signaling. Plant Physiology **117,** 113–121.

Uggla C, Moritz T, Sandberg G, Sundberg B. 1996. Auxin as a positional signal in pattern formation in plants. Proceedings of the National Academy of Sciences, USA **93,** 9282–9286.

Vaganov EA, Anchukaitis KJ, Evans MN. 2011. How well understood are the processes that create dendroclimatic records? A mechanistic model of the climatic control on conifer tree-ring growth dynamics. In Hughes MK, Swetnam TW, Diaz HF, eds. Dendroclimatology: progress and prospects. In: Dordrecht: Springer Netherlands, 37–75.

Vaganov EA, Hughes MK, Shashkin AV. 2006. Growth dynamics of conifer tree rings: images of past and future environments. Ecological studies. Berlin, Heidelberg: Springer.

Vieten A, Vanneste S, Wisniewska J, Benková E, **Benjamins R, Beeckman T, Luschnig C, Friml J.** 2005. Functional redundancy of PIN proteins is accompanied by auxin-dependent cross-regulation of PIN expression. Development **132,** 4521–4531.

Wartlick O, Kicheva A, González-Gaitán M. 2009. Morphogen gradient formation. Cold Spring Harbor Perspectives in Biology **1,** a001255.

Wilkinson S, Ogée J, Domec JC, Rayment M, Wingate L. 2015. Biophysical modelling of intra-ring variations in tracheid features and wood density of *Pinus pinaster* trees exposed to seasonal droughts. Tree Physiology **35,** 305–318.

Willis L, Refahi Y, Wightman R, Landrein B, Teles J, Huang KC, Meyerowitz EM, Jönsson H. 2016. Cell size and growth regulation in the *Arabidopsis thaliana* apical stem cell niche. Proceedings of the National Academy of Sciences, USA **113,** E8238–E8246.

Wilson BF. 1984. The growing tree. Amherst: University of Massachusetts Press.

Yeoman MM, Brown R. 1971. Effects of mechanical stress on the plane of cell division in developing callus cultures. Annals of Botany **35,** 1102–1112.

Ziaco E, Biondi F, Rossi S, Deslauriers A. 2016. Environmental drivers of cambial phenology in Great Basin bristlecone pine. Tree Physiology **36,** 818–831.